Revista Brasileira de Climatologia
Brazilian Journal of Climatology

OPEN ACCESS

DOI: 10.5380/abclima

CLIMATIC VARIABILITY OF THE SOUTH PACIFIC OCEAN DURING 1900–2010 IN THE ENVIRONMENTAL RECORDS OF WEST ANTARCTICA

VARIABILIDADE CLIMÁTICA DO OCEANO PACÍFICO SUL DURANTE 1900–2010 NOS REGISTROS AMBIENTAIS DA ANTÁRTICA OCIDENTAL

VARIABILIDAD CLIMÁTICA DEL OCEANO PACÍFICO SUR DURANTE 1900–2010 EN LOS REGISTROS AMBIENTALES DE LA ANTÁRTIDA OCCIDENTAL

José Mauro Dalla Rosa
Universidade Federal do Rio Grande do Sul
jmaurodallarosa@gmail.com

Jefferson Cardia Simões
Universidade Federal do Rio Grande do Sul
jefferson.simoes@ufrgs.br

Pedro Amaral Reis
Universidade Federal do Rio Grande do Sul
pamaralreis@gmail.com

Francisco Eliseu Aquino
Universidade Federal do Rio Grande do Sul
francisco.aquino@ufrgs.br

Isaías Ullmann Thoen
Universidade Federal do Rio Grande do Sul
isaias.thoen@ufrgs.br

Ronaldo Torma Bernardo
Universidade Federal do Rio Grande do Sul
rtbernardo12@gmail.com

Jeffrey Daniel Auger
Universidade Federal do Rio Grande do Sul
jauger83@gmail.com

Abstract: In this work, we present the climatic evolution of the South Pacific Ocean from 1900 to 2010 and its environmental influence over West Antarctica. We analyzed the sea surface temperature, mean sea level pressure, and meridional wind (850 hPa) of the South Pacific Ocean using ERA-20C reanalysis (European Center for Medium-Range Weather Forecasts), and compared these parameters with the regional temperature obtained indirectly (by proxy) from two ice cores from the West Antarctic ice sheet (Mount Johns and Ferrigno). The sea surface temperature increased in almost the entire South Pacific Ocean from 1900 to 2010; in the equatorial Pacific, it increased by 2.1 °C from 1916 to 1997, while in the middle latitudes of the South Pacific, it increased by 1.1 °C from 1923 to 2001. This increase occurred concurrently with a positive trend in the Southern Annular Mode and a change the mean sea level pressure anomaly from 1960 onwards. This atmospheric pressure increased at middle latitudes and decreased around Antarctica in the circumpolar low-pressure zone, strengthening the Amundsen Sea Low and changing the pattern of the meridional wind anomaly (850 hPa) between medium and high latitudes in the South Pacific. Furthermore, since 1960, a greater flow from north to south (onshore) has predominated from the southeast South Pacific to the north of West Antarctica. Such changes caused a reduction in the sea ice extent in the Amundsen and Bellingshausen Seas and an increase in average atmospheric temperature primarily in the coastal region of West Antarctica, as demonstrated by the Ferrigno ice core record. Conversely, the Mount Johns region did not show the same trend in atmospheric temperature, as it was influenced mainly by cold air masses from the Antarctic ice sheet.
Keywords: South Pacific Ocean. West Antarctica. Climatology.

Resumo: Nesse trabalho, apresentamos a evolução climática do Oceano Pacífico Sul entre 1900 e 2010 e seu papel ambiental sobre a Antártica Ocidental. Analisamos a temperatura da superfície do mar, pressão média ao nível do mar, e vento meridional (850 hPa) do Oceano Pacífico Sul usando reanálises ERA-20 (*European Centre for Medium-Range Weather Forecasts*), e comparamos esses parâmetros com a temperatura regional obtida indiretamente (por *proxys*) de dois testemunhos de gelo (Monte Johns e Ferrigno) do manto de gelo Antártico Ocidental. A temperatura da superfície do mar aumentou em praticamente todo o oceano Pacífico Sul entre 1900 e 2010, no Pacífico Equatorial aumentou 2,1°C entre 1916 e 1997, enquanto nas latitudes médias do Pacífico Sul o aumento foi de 1,1°C entre 1923 e 2001. Este aumento ocorreu concomitantemente à tendência positiva do Modo Anular Sul e uma mudança do sinal da anomalia da pressão média ao nível do mar a partir principalmente de 1960. Aumentando a pressão atmosférica em latitudes médias e diminuindo ao redor da Antártica na zona de baixa pressão circumpolar, fortalecendo a baixa do Mar de Amundsen e mudando então o padrão da anomalia do vento meridional (850 hPa) entre latitudes médias e altas no Pacífico Sul. A partir de 1960 predominou um maior escoamento de norte para sul (*onshore*) do sudeste do Pacífico Sul para o norte da Antártica Ocidental. Tais mudanças resultaram na redução na extensão do gelo marinho nos mares de Amundsen e Bellingshausen e na elevação na temperatura atmosférica média principalmente na região costeira da Antártica Ocidental, como demonstrado pelo registro do testemunho de gelo Ferrigno. Já a região do Monte Johns não mostra a mesma tendência na temperatura atmosférica, pois sofre maior influência de massas de ar frias do interior do manto de gelo Antártico.
Palavras-chave: Oceano Pacífico Sul. Antártica Ocidental. Climatologia.

Resumen: En este trabajo, presentamos la evolución climática del Oceano Pacífico Sur desde 1900 y 2010 y su influencia ambiental sobre la Antártica Occidental. Analizamos la temperatura de la superficie del mar, la presión media al nivel del mar, y el viento meridional (850 hPa) del Oceano Pacífico Sur utilizando el reanálisis ERA-20C (*European Centre for Medium-Range Weather Forecasts*), y comparamos estos parámetros con la temperatura regional obtenida indirectamente (por *proxys*) de dos núcleos de hielo de la capa de hielo de la Antártida Occidental (Monte Johns y Ferrigno). La temperatura de la superficie del mar aumentó en prácticamente todo el oceano Pacífico Sur entre

1900 y 2010, en el Pacífico Ecuatorial aumentó 2,1 °C entre 1916 y 1997, mientras que en las latitudes medias del Pacífico Sur el aumento fue de 1,1 °C entre 1923 y 2001. Este aumento se produjo al mismo tiempo que una tendencia positiva del Modo Anular Sur y un cambio en el señal de la anomalía de la presión media al nivel del mar desde principalmente 1960, aumentando la presión atmosférica en latitudes medias y disminuyendo alrededor de la Antártida en la zona de baja presión circumpolar. Fortaleciendo la baja del Mar de Amundsen y cambiando el patrón de la anomalía del meridional (850 hPa) entre latitudes medias y altas en el Pacífico Sur. Desde 1960, ha predominado un mayor flujo de norte a sur (*onshore*) desde el sureste del Pacífico Sur hasta el norte de la Antártida Occidental. Dichos cambios provocaron una reducción en la extensión del hielo marino en los mares de Amundsen y Bellingshausen y un aumento en la temperatura atmosférica promedio principalmente en la región costera de la Antártica Occidental, como lo demuestra el registro del núcleo de hielo de Ferrigno. La región de Mount Johns, por otro lado, no muestra la misma tendencia en la temperatura atmosférica, ya que fue influenciada por masas de aire frío desde dentro de la capa de hielo Antártica.

Palablas-clave: Oceano Pacífico Sur. Antártica Occidental. Climatologia.

Submetido em: 08/10/2020
Aceito para publicação em: 26/07/2021
Publicado em: 22/09/2021

INTRODUCTION

Antarctica and the South Pacific Ocean (SPO) are the main climatic regulators of the Southern Hemisphere (SH). The Amundsen Sea Low (ASL), located between the South Pacific and West Antarctica, is the main climatic driver responsible for temperature and humidity exchange from the SPO intermediate latitudes and the Antarctic continent (BROMWICH et al., 2013; TURNER et al., 2013). The climatic variability of the SPO plays an important role over the ASL region (TURNER et al., 2013) because of atmospheric teleconnections caused by Rossby waves and large-scale variability modes such as the Southern Annular Mode (SAM), El-Niño Southern Oscillation (ENSO), and Pacific South American Mode (PSA). A positive trend in SAM since 1960 (THOMPSON and SOLOMON, 2002; MARSHALL, 2003) resulted in more cyclogenesis south of the SPO, a shift of the polar jet stream poleward, and the deepening of the ASL (TURNER et al., 2009; RAPHAEL et al., 2016). This has contributed to a higher advection of hot air masses originating in the South/Southeast Pacific to the interior of West Antarctica, causing changes in the average air temperature, sea ice extent, snow accumulation, and mass balance of the ice region (TURNER et al., 2013; MAYEWSKI et al., 2017).

The West Antarctic Ice Sheet (WAIS) is potentially unstable, and changes in dynamics, mass balance, and retraction of its glacier fronts in the last decades, as a response to the South Pacific climatic variability have been identified in recent studies (DING et al., 2011; HOLLAND et al., 2020). As the WAIS is primarily grounded below sea level, the dynamic instability of this ice mass could cause a rapid collapse (over a period ranging from decades to centuries) and a significant increase in the mean sea level (BROMWICH et al., 2013; MAYEWSKI et al., 2013; THOMAS et al., 2015).

The isotopic composition of Antarctic snow and ice (measurement of the deuterium/hydrogen and $^{18}O/^{16}O$ ratios), along with the ionic and trace element contents, provide proxies for the climatic variability of the South/Southeast Pacific Ocean. They are essential tools for investigating past environmental variability because meteorological data are too recent, scarce, and restricted to a few sites on the Antarctic continent and SPO, which complicates environmental analysis. Climatic reanalyses of the 20th century, such as the ERA-20C (European Center for Medium-Range Weather Forecasts - ECMWF), are also crucial for reconstructing the climatology of the SH for periods of time before remote sensing (BROMWICH et al., 2013; STEIGt et al., 2013; THOMAS et al., 2013; POLI et al., 2015).

In this study, we investigated the climatic variability of the SPO between 1900 and 2010 and its role in the West Antarctic (WA) climate using ERA-20C reanalysis and proxies from two ice cores collected in Mount Johns (79°55' S, 94°23' W; 2100 m altitude) and Ferrigno (74°34' S, 86°54' W; 1354 m altitude) (Figure 1).

Figure 1 – Location of the two ice core sites used in this work, drilled in West Antarctica: Mount Johns (green triangle, 79°55' S, 94°23' W) and Ferrigno (red triangle, 74°34' S, 86°54' W).

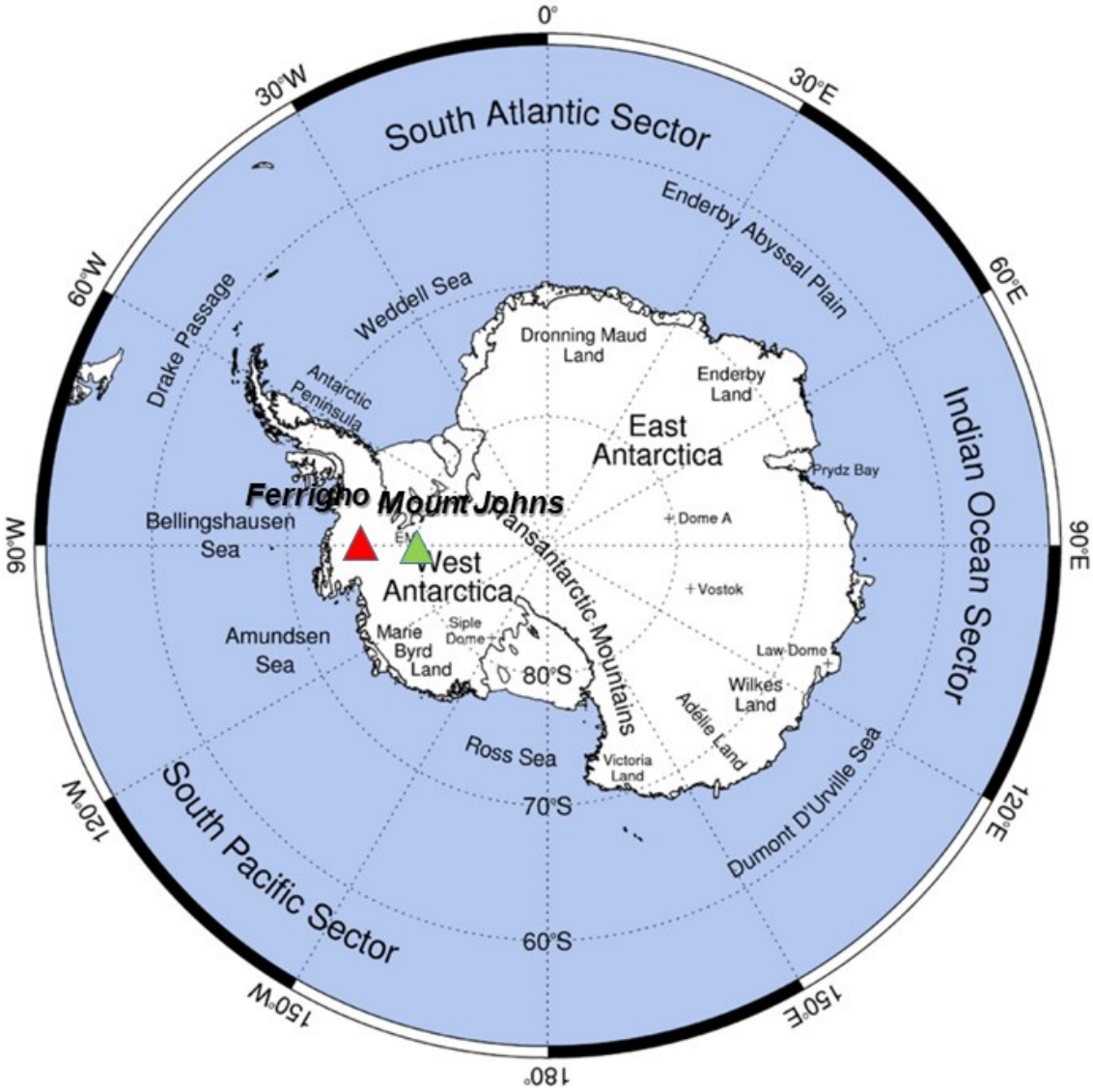

Source: Modified from SCAR (2014).

MATERIALS AND METHODS

ERA-20C climatic reanalysis

The ERA-20C reanalysis was developed by the ECMWF and is a global climate reanalysis that spans the 1900–2010 period (POLI et al., 2016). ERA-20C uses a coupled atmosphere/land-and-sea surface model with meteorological observations of the surface. The primary difference between ERA-20C and ERA-Interim (BERRISFORD et al., 2011) is the time span, as ERA-20C includes data before 1979, when no satellite observation data existed and meteorological data were primarily observational from stations and ships (POLI et al., 2015, 2016).

We used the following ERA-20C parameters for our work: sea surface temperature (SST, in Celsius (°C)), mean sea level pressure (MSLP, in hPa), and meridional wind at 850 hPa (V, in m s^{-1}). The ERA-20C SST is from the Hadley Centre Sea Ice and Sea Surface Temperature dataset (HadISST-2.1.0.0), a database of reconstructions spanning 1899–2010 (POLI et al., 2015). We used a spatial resolution of 0.5° between 10°N and 90°S to investigate the climatic variability in the SPO during the 1900–2010 period and calculated anomalies for the cited parameters at 20-year intervals based on the climatology from 1900 to 2010.

Glaciochemical analysis

For our glaciochemical analysis, we used data from the top 46 m of the Mount Johns ice core, drilled during the 2007–2008 austral summer in the Pine Island Glacier (in the WA). The core was dated using the seasonal variability of non-sea salt sulfate ($nssSO_4^{2-}$), with peak concentrations during the austral summer, and sodium (Na^+), with peak concentrations in austral winter (THOEN et al., 2018). Oxygen stable isotopes ($\delta^{18}O$), used to estimate atmospheric temperatures at the drilling site, were determined using a wavelength-scanned cavity ring-down spectroscopy WS-CRDS (model L2130-i, Picarro Inc., US) (SCHWANCK et al., 2017; THOEN et al., 2018). Interpretation of the environmental records was carried out using two proxies: Na^+ and $\delta^{18}O$. We also used δD data from the Ferrigno ice core analyzed by Thomas et al. (2013), from 1900–2010, for comparison with the Mount Johns $\delta^{18}O$ record. The Ferrigno ice core $\delta^{18}O$ record was accessed at

https://ramadda.data.bas.ac.uk/repository/entry/show/?entryid=6ffa3d36-a521-44f7-9e12-213458dafce3

RESULTS

South Pacific Ocean climatology between 1900 and 2010

In the tropics, heat transport from the ocean to the atmosphere via evaporation is the primary contributor to large-scale atmospheric teleconnections around the globe (TRENBERTH, 2011; CHENG et al., 2019). In addition to driving the atmospheric circulation of the Walker and Hadley cells, the anomalous latent heat in the tropics, associated with intense convection, also contributes to the generation and propagation of Rossby waves on a global scale, controlling storm tracks (TRENBERTH, 2011; CHENG et al., 2019).

Figure 2 shows the SST variability for the SH (focusing on the SPO) between 1900 and 2010 from the ERA-20C reanalysis (every 20 years). We see a gradual and geographically broad increase in the SPO SST over the 110 years studied. From 1900 to 1940 (Figure 2a, 2b), there was a predominance of SST negative anomalies, with one exception in the SPO southeast region (e.g., north of the WA), where a positive anomaly is visible (although this could likely be attributed to a reanalysis error for the region). From 1940 onward, the negative anomalies observed earlier started to change to positive anomalies and warming became visible from 1981 to 2010 in the intermediate latitudes of the SPO (Figures 2e, 2f), specifically east of New Zealand.

Figure 2 – Annual SST anomaly (°C) between 1900–2010 divided in 20-year periods*: (a) 1900–1920; (b) 1921–1940; (c) 1941–1960; (d) 1961–1980; (e) 1981–2000; (f) 2001–2010. *Except for 1900–1920 (21-year period) and 2001–2010 (10-year period).

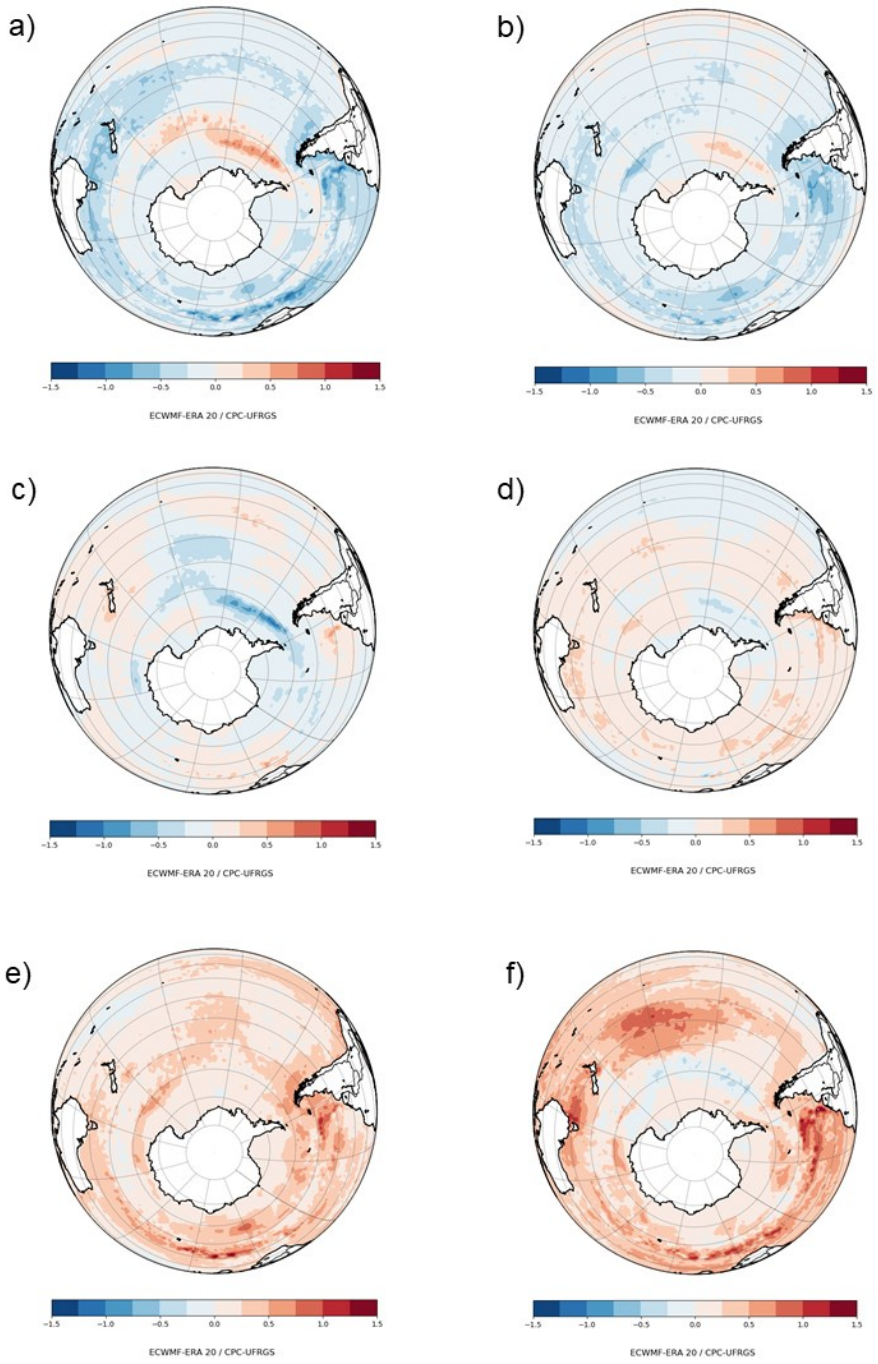

Source: ECMWF and Centro Polar e Climático - Universidade Federal do Rio Grande do Sul (CPC-UFRGS).

Figure 3 shows the SST trend in latitudinal zones derived from the ERA-20C reanalysis between 10°N and 10°S, 40°S and 60°S, and 30°S and 60°S (SST anomaly produced by NOAA*). All sectors of the SPO show a trend of increasing SST for 1900–2010 (Table 1). In the equatorial region (between 10°N and 10°S), we observed an increasing trend of +0.007 °C yr^{-1} for the

1900–2010 period, and a maximum average value of 28.4 °C in 1997. Between 40°S and 60°S, the SST trend is + 0.008 °C yr^{-1} with a maximum average of 12.6 °C in 2001. For these latitudes, the warming trend began in the 1930s (Figure 3b and 3c).

Figure 3 – Mean SST for the SPO latitudinal zones derived from ERA-20C for the 1900–2010 period between (a) 10° N and 10° S; (b) 30° S and 60° S*; and (c) 40° S and 60° S.

* SST anomaly produced by NOAA for the entire globe at these latitudes.

https://www.ncei.noaa.gov/data/noaa-global-surface-temperature/v5/access/timeseries

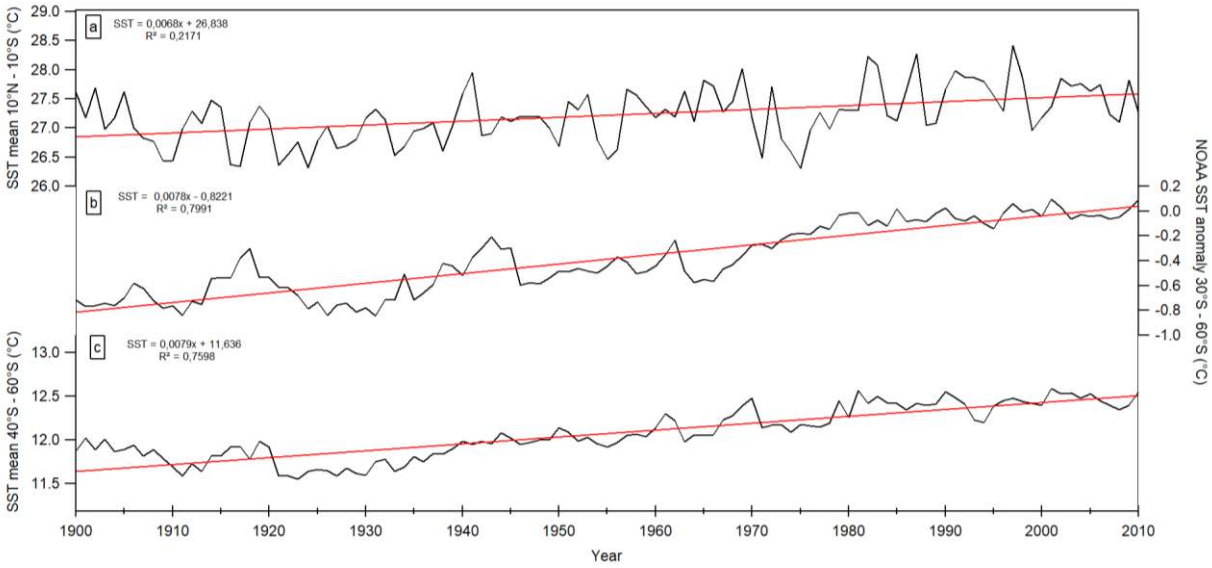

Source: Elaborated by the authors (2020)

Although there has been general warming in the SPO during the 1900–2010 period, the region east of New Zealand (40° S, 150° W) showed a higher SST increase (+ 0.008 °C yr^{-1}, Figure 4b). The amplitude was also the highest (2.3 °C), with an average minimum of 11.8 °C in 1911 and an average maximum of 14.1 °C in 2004. On the Equatorial region (10°S, 120°W), the warming trend was lower (+ 0.003 °C yr^{-1}), with an amplitude of 1.8 °C, a minimum of 23.8 °C in 1955, and a maximum of 25.6 °C in 1983 (Figure 4a).

Table 1 – Sea surface temperature (SST) statistics (in °C) for different latitudinal bands and locations in the SPO between 1900 and 2010 (annual trend).

SST (°C)	MIN	MAX	AVERAGE	AMPLITUDE	TREND	STANDARD DEVIATION
10°N–10°S	26.3	28.4	27.2	2.1	+ 0.007	0.5
40°S–60°S	11.5	12.6	12.1	1.0	+ 0.008	0.3
10°S, 120°W	23.8	25.6	24.6	1.8	+ 0.003	0.3
40°S, 150°W	11.8	14.1	12.8	2.3	+ 0.008	0.4

Source: Elaborated by the authors (2020)

Figure 4 – Average sea surface temperature (SST, in °C) derived from ERA-20C reanalysis between 1900 and 2010 for points located in the SPO. Coordinates (a) 10° S, 120° W; and (b) 40° S, 150° W.

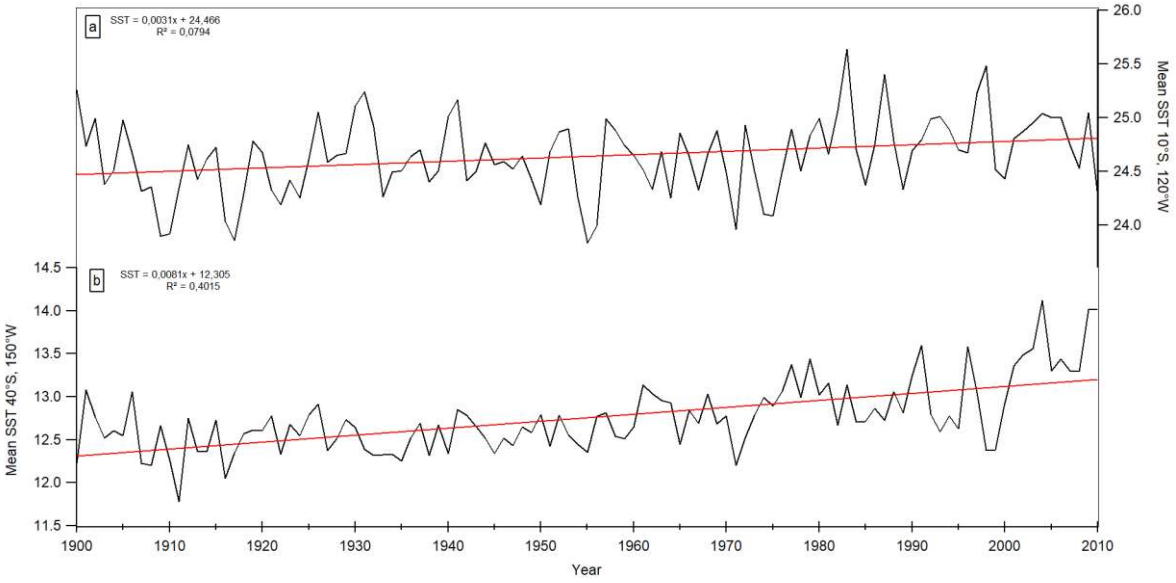

Source: Elaborated by the authors (2020)

Figure 5 shows the behavior of the SPO mean atmospheric sea level pressure between 1900 and 2010 every 20 years. There was a gradual but unmistakable change in the MSLP trend from 1900–2010 in the SH, with a prevailing positive anomaly at high latitudes (~60°S) and a negative anomaly at intermediate latitudes (~40°S) at the beginning of the 20th century. Then, there was a gradual inversion of these anomalies the end of the 20th century/beginning of the 21st century.

In the 1900–1920 period, there was a positive MSLP anomaly north of WA and a negative MSLP anomaly east of New Zealand (Figure 5a). In the 2001–2010 period, in the region north of WA, the MSLP shifted to a negative anomaly, and the central region of the SPO showed a positive anomaly at intermediate latitudes (Figure 5f). Finally, the 1941–1980 period marked a transition, with moderate MSLP anomalies over the SPO (Figures 5c and 5d).

This shift in the MSLP anomaly pattern between intermediate (~40° S) and high (~60° S) latitudes during the 20th century and beginning of the 21st century also indicated a shift in SAM signal from a negative phase in the early 20th century to a positive phase from the 1960s onward. This positive SAM trend strengthened the temperature gradient at higher SH latitudes, intensifying the jet stream and westerlies toward the pole and influencing temperatures in the Antarctic continent (THOMPSON and SOLOMON, 2002; MARHALL, 2003; JONES et al., 2009; ABRAM et al., 2014).

Figure 5 – MSLP annual anomaly (in hPa) between 1900 and 2010 divided in 20-year periods*: (a) 1900–1920; (b) 1921–1940; (c) 1941–1960 (d) 1961–1980; (e) 1981–2000; (f) 2001–2010. *Except for 1900–1920 (21-year period) and 2001–2010 (10-year period).

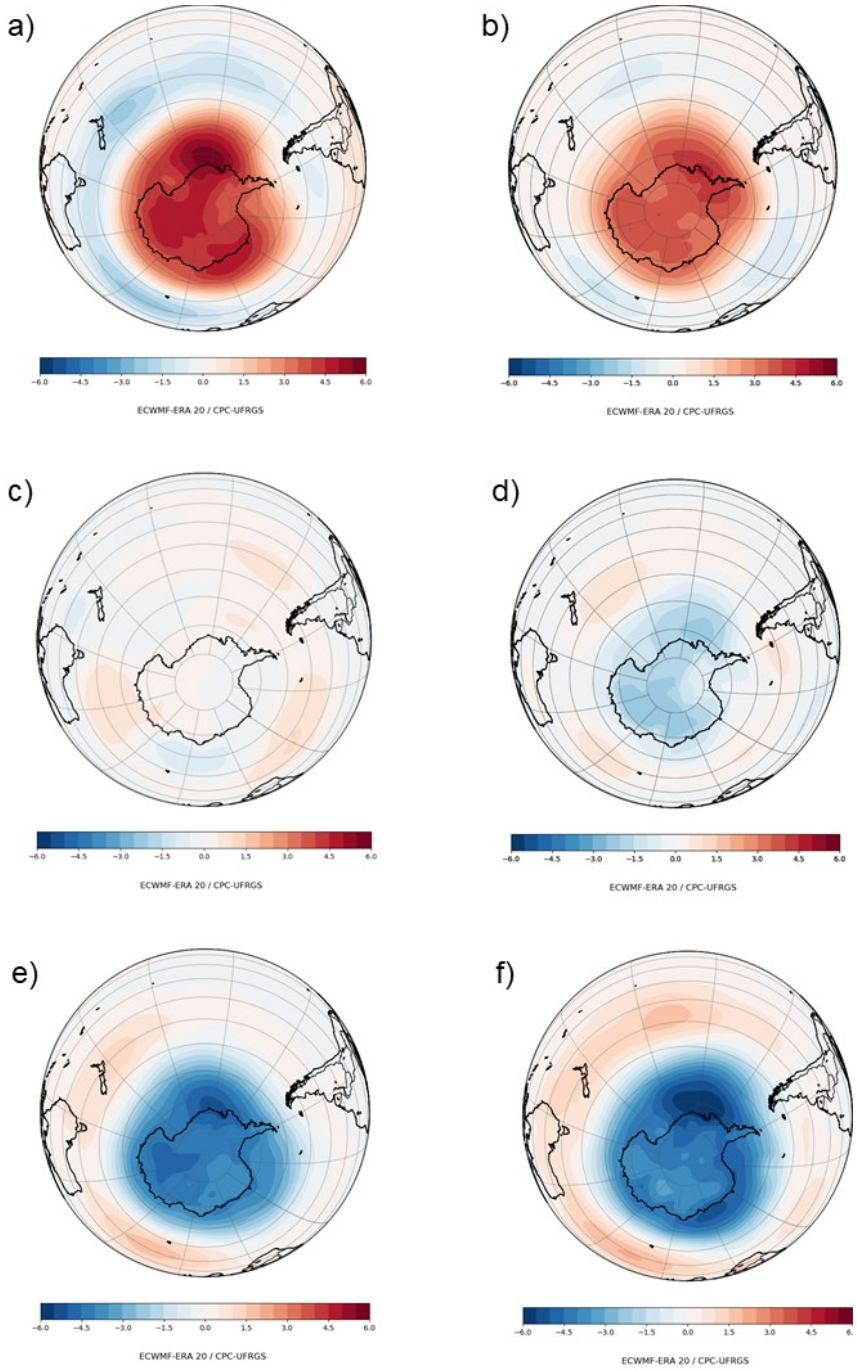

Source: Elaborated by the authors (2020)

Concomitantly with the signal shift in the SPO MSLP, we also noted a change in the anomaly pattern of the meridional wind (v) at 850 hPa between intermediate and high latitudes (40° S–60° S) in the period studied (1900–2010) (Figure 6). In the early 20th century (1900–1920), the meridional wind anomaly was predominantly positive, from south to north

(offshore), from the northern part of the WA to the Austral Ocean (Amundsen and Bellingshausen Seas) and southeast of the Pacific Ocean (Figure 6a). However, in the Ross Sea region, northwest of WA, we noted a negative anomaly in the meridional wind (north/south) for the 1900–1920 period from the SPO intermediate latitudes to the interior of WA (onshore) through the Ross Ice Shelf.

At the beginning of the 20th century, this meridional wind pattern showed a prevalence of atmospheric flow from south to north (cold and dry air) from the WA to the Bellingshausen Sea. In contrast, a higher atmospheric flow and transport of heat and humidity occurred from the intermediate latitudes of the SPO to the Ross Ice Shelf. Figure 6b (1921–1940) shows the same meridional wind anomaly pattern observed for 1900–1920 but weaker. Between 1941 and 1960 (Figure 6c), no pattern was observed for the meridional wind in the SPO.

In the 1961–1980 period, the meridional wind pattern started to change. North of WA, in the Bellingshausen Sea, the anomaly showed an opposite signal compared to earlier periods, prevailing a higher atmospheric flow from north to south (onshore), from southeast of the SPO to north of WA. In the Ross Sea region, we observed a positive anomaly (south/north), favoring the atmospheric flow from the WA (cold/dry) to the Austral Ocean (Ross Sea). This meridional wind flow pattern continued until the end of the 20th and into the 21st century.

Environmental record in West Antarctica

Snow preservation in polar regions ensures an excellent record of paleoenvironmental conditions. Detailed chemical and physical analyses of snow, firn[1], and ice from cores drilled in the polar ice sheets (Antarctica and Greenland) provide paleoclimatic data for the last 800000 years (WOLFF, 2012).

The analysis of stable isotopes from ice cores, for example, has been widely used for relative dating and to estimate the temperature in polar regions since the pioneering work of Dansgaard (1964). The ratio of stable isotopes from ice cores (δD e $\delta^{18}O$) is an important "tool" to measure the temporal and seasonal variability of temperature in the polar regions, allowing us to differentiate summer precipitations from winter ones (interannual variability), warm

[1] **Firn** – Intermediate state between snow and ice (SIMÕES, 2004).

eras from cold ones (millennial variability), and consequently differentiate glacial and interglacial cycles (WOLFF, 2012). According to Petit et al. (1999), data from the Vostok ice core (70°28'S, 106°48'E) show that the isotopic ratios of $\delta^{18}O$ and δD in East Antarctica are linearly correlated with the snow precipitation temperature. Therefore, stable isotopes are usually used as temperature proxies (BROOK and BUIZERT, 2018).

Figure 6 – Meridional wind annual anomaly at 850 hPa (v) between 1900 and 2010 divided in 20-year periods*: (a) 1900–1920; (b) 1921–1940; (c) 1941–1960; (d) 1961–1980; (e) 1981–2000; (f) 2001–10.
*Except for 1900–1920 (21-year period) and 2001–2010 (10-year period).

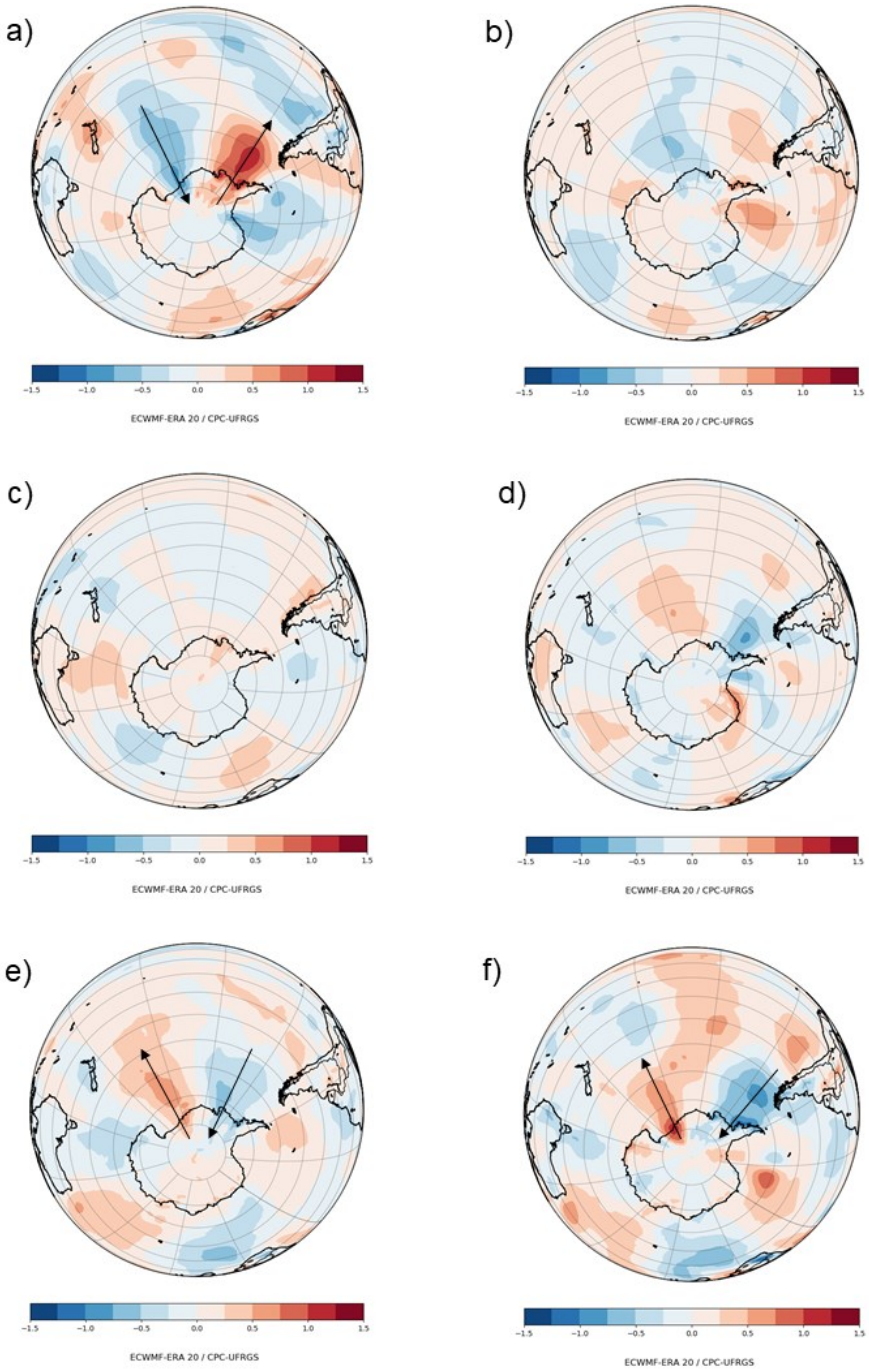

Source: Elaborated by the authors (2020)

Ice cores also provide particulate matter (aerosols) data, from microparticles to chemical species, as significant ions and trace elements. They are deposited along with snow in the polar regions and show variability at different timescales due to local to global environmental changes (LEGRAND and MAYEWSKI, 1997; WOLFF, 2012). Furthermore, the seasonal cycle of each ionic species deposited (cations and anions, such as Na^+, K^+, Mg^{2+}, Ca^{2+}, MSA, Cl^-, $N0_3^-$, and $S0_4^{2-}$) provides information about air mass source regions, transport pathways, and transport intensity, among others (LEGRAND and MAYEWSKI, 1997; WOLFF, 2012).

For example, marine (sea salt) and continental aerosols in the Vostok ice core show higher concentrations during glacial periods compared to interglacial periods and are negatively correlated with temperature. In the present, marine aerosol concentrations in the Antarctic peak during winter and spring, concomitant with the highest sea ice extension in the SH (LEGRAND and MAYEWSKI, 1997; PETIT et al., 1999).

The 108-year record of oxygen ($\delta^{18}O$) and sodium (Na^+) from the Mount Johns ice core, as well as the 110-year record of hydrogen (δD) from the Ferrigno ice core, are shown in Figure 7. Comparing trends of $\delta^{18}O$ from Mount Johns and δD from Ferrigno, we observed an increasing trend (δD) in the latter, while in the former ($\delta^{18}O$), this trend was not observed (Figure 7).

Sodium concentrations in the Mount Johns core (Figure 7a) showed a decreasing trend during the study period (- 0.083 µg L yr^{-1}). Between 1902 and 1932, the average annual values were approximately 22 µg L^{-1}, increasing to nearly 30 µg L^{-1} between 1932 and 1943. From then on, concentrations decreased, reaching a minimum value of 8.6 L^{-1} in 2005. Figure 7b shows the average annual values of $\delta^{18}O$ from Mount Johns. Oxygen isotopic ratios varied around the average (- 36.20 ‰); we did not find any statistically significant trend for this record. Figure 7c shows the δD record from the Ferrigno ice core (analyzed by Thomas et al., 2013), showing an increasing trend in the isotopic ratios along with the profile (+ 0.078 ‰ yr^{-1}), especially from 1960 onwards.

Figure 7 – (a) Sodium (Na^+) and (b) Oxygen isotopic record ($\delta^{18}O$) from Mount Johns, and (c) Hydrogen isotopic record (δD) from Ferrigno, both cores from West Antarctica.

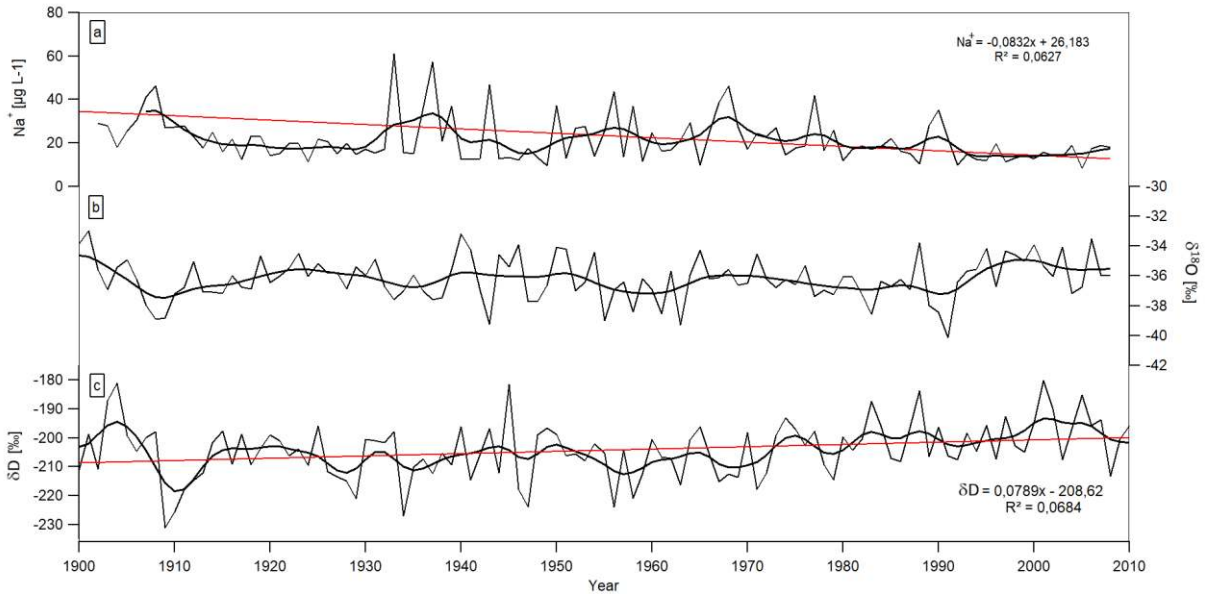

Source: Elaborated by the authors (2020)

DISCUSSION

Warming in the tropics controls atmospheric circulation on a large scale through teleconnections caused mainly by heat loss from the ocean to the atmosphere via evaporation (TRENBERTH, 2011; CHENG et al., 2019).

Changes in the thermic structure of the atmosphere result from the direct radiative effect and variations in the SST. The temperature increase in the equatorial and tropical regions alters the atmosphere's thermic structure, leading to the strengthening and expansion of the Hadley cell toward the South Pole (HUDSON, 2012; HU et al., 2018).

A possible strengthening of the Hadley cell occurred due to an increasing SST in the tropics between 1900 and 2010 (Figure 2) and the consequent atmospheric heating transporting energy to the subtropics, strengthening the descending branch of the Hadley cell (LIU and ALEXANDER, 2007). This increased the atmospheric pressure in the SPO intermediate latitudes, reduced precipitation and cloud quantity, and increased the incidence of short-wave solar radiation in the region, increasing the air temperature and SST, as observed in the region east of New Zealand (Figure 8).

The link between the tropical SST and remote areas described as 'atmospheric bridges' could result in changes in the ocean surface heat flux due to modifications in the Walker and

Hadley cell circulation, which could act as a Rossby wave generator at high latitudes (LIU and ALEXANDER, 2007). In addition, the convection area in the tropical Pacific shifts from Indonesia during La Niña events to the proximities of the International Date Line during El Niño events. Thus, the ENSO response in intermediate latitudes varies according to its warming and cooling phases, which influence and modulate subtropical anticyclones (TURNER, 2004; YUAN et al., 2018).

Figure 8 – Correlation between ERA-Interim (ECMWF) air temperature at 2 m (T2) and SST at 40° S, 150° W (SPO), derived from ERA-20C reanalysis (ECMWF) for the 1979–2000 period. Significance level of 0.95.

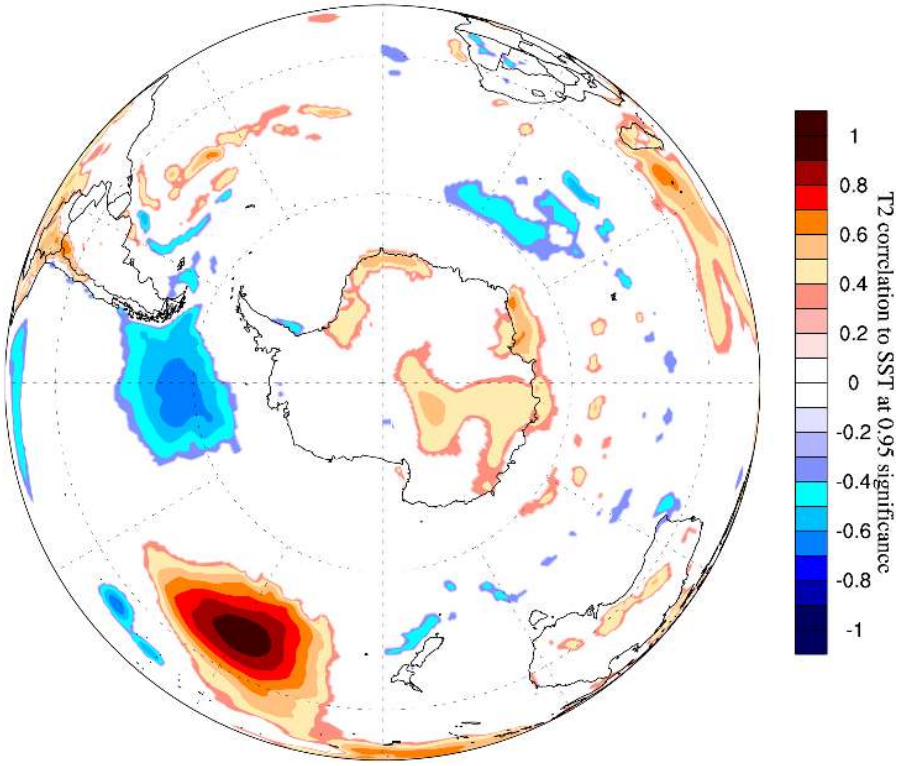

Source: Climate Change Institute (CCI) of the University of Maine (UMaine) / ECMWF / CPC-UFRGS. https://traveler.um.maine.edu/reanalysis/monthly_correl/

Several studies (MARSHALL, 2003; NICOLAS and BROMWICH, 2011; THOMPSON et al., 2011; ABRAM et al., 2014) found a positive SAM phase in the last decades, mainly after 1960. This positive phase is highlighted during autumn (m-a-m) and summer (d-j-f) and is also attributed to stratospheric ozone destruction. This trend leads to a strengthening of the atmospheric pressure in intermediate latitudes (~40° S), reduction of the atmospheric pressure around Antarctica (~65° S), and intensification and shift of the westerlies and storm

tracks around Antarctica toward the pole (MARSHALL, 2003; NICOLAS and BROMWICH, 2011; THOMPSON et al., 2011; ABRAM et al., 2014).

The expansion of the Hadley cell toward the pole in conjunction with the positive SAM trend since the 1960s contributed to strengthening the MSLP in the SPO intermediate latitudes during the same period (Figure 5). A higher MSLP in the SPO increased the meridional flow and intensified heat and moisture transport from the SPO intermediate latitudes to the Antarctic circumpolar low zone (Figures 9a, b).

Figure 9 – Correlation between (a) ERA-Interim (ECMWF) geopotential height at 500 mb and SST (°C); and (b) ERA-Interim meridional wind at 10 m (V10) and SST (°C). Both correlations are derived from ERA-20C (ECMWF), for the coordinates 40° S, 150° W (on the SPO), for the 1979–2010 period, at a 0.95 significance level.

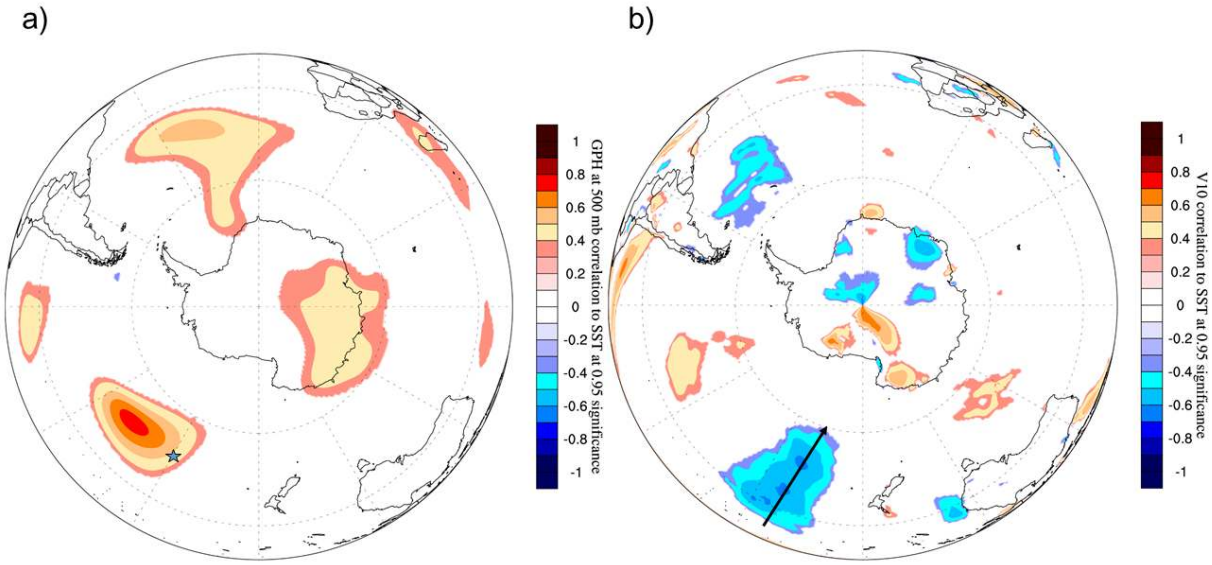

Source: CCI-U.MAINE / ECMWF / CPC-UFRGS.
https://traveler.um.maine.edu/reanalysis/monthly_correl/

This meridional flow contributed to the strengthening of the ASL since around the 1960s (Figure 5d), controlling the meridional atmospheric circulation, which regulates the heat and moisture transport to the interior of Antarctica, mainly to the west of WA. Figure 10 shows an inverse correlation between the ASL and the region east of New Zealand in the SPO (40° S, 150° W), where there is a significant SST anomaly. Thus, the ASL is an essential component of the meridional circulation between intermediate and high latitudes of the SPO, linking the tropical Pacific with the Austral Ocean (HOSKING et al., 2013; RAPHAEL et al., 2016).

The meridional wind pattern in the Bellingshausen Sea region, north of WA (Figure 6), shifted from a south-north atmospheric flow at the beginning of the 20th century (cold and dry winds from WA towards the Bellingshausen Sea, Figure 6a) to a north-south flow around 1960 (onshore, from the southeast SPO towards the northern region of WA, Figure 6d). This was driven by a reduction in the MSLP in the Antarctic low-pressure circumpolar zone and a deepening of the ASL due to the positive SAM trend during the same period (THOMPSON and SOLOMON, 2002; MARSHALL et al., 2006).

The atmospheric flow pattern and the synoptic activity (originating in the southeast SPO) moving toward the pole, associated with the ASL variation, influence the environmental and climatic properties of the WAIS. Thus, the ASL deepening since the 1960s increased the flow of warm and humid air onshore from the southeast SPO to WA (north to south) (HOSKING et al., 2013; RAPHAEL et al., 2016). An increase in meridional flow favors aerosol advection from the Amundsen/Bellingshausen Seas, which are then deposited and preserved in snow and ice layers in the WAIS.

Figure 10 – Correlation between ERA-Interim (ECMWF) MSLP and ASL (http://www.antarctica.ac.uk/data/absl/) for 1979–2010 with a significance level of 0.95.

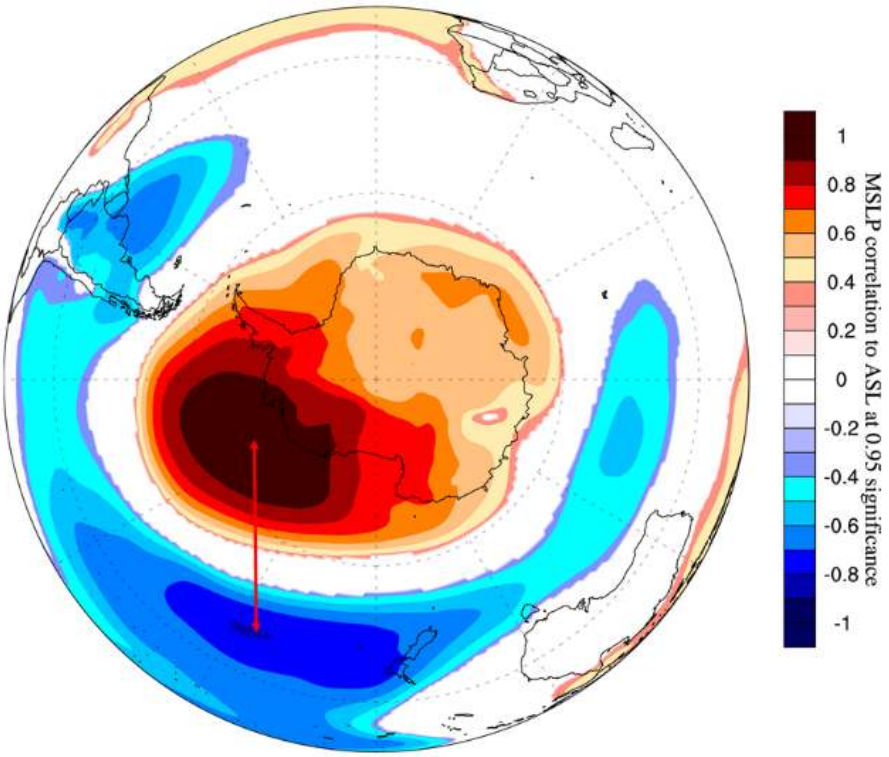

Source: CCI-U.MAINE / ECMWF / CPC-UFRGS.

Using data from an ice core drilled in the WAIS divide, Steig et al. (2013) observed that the $\delta^{18}O$ ratios increased concomitantly with the temperature in the region over the last 50 years. The positive trend in $\delta^{18}O$ increased when anomalous atmospheric flow occurred from north to south, between the southeast SPO and WA.

The glaciochemical data used in this study (Figure 7) revealed a reduction in Na^+ concentrations (- 0.083 µg L^{-1} yr^{-1}) in the Mount Johns drilling site; however, the $\delta^{18}O$ ratios remained stable during the study period. Nonetheless, the Ferrigno δD record showed an increasing trend (+ 0.078‰ yr^{-1}) during the same period.

Frost flower crystals are the primary source of Na^+ in Antarctica during austral winter (WOLFF et al., 2003; INOUE et al., 2017). According to Mayewski et al. (2017), an increase (decrease) in Na^+ indicates a higher (lower) atmospheric flow toward the pole, controlled by the deepening (weakening) of the Antarctic circumpolar low and the ASL. As a decrease in sodium concentrations in the Mount Johns ice core was observed with stable $\delta^{18}O$ ratios, it was concluded that there was a reduction in sea ice extent (source of frost flowers) in the Amundsen/Bellingshausen seas during the study period, according to Schwanck et al. (2017). This is valid considering that a higher atmospheric flow would have also increased the isotopic ratios.

Nonetheless, closer to the coast, the Ferrigno site shows that the region had a more significant influence from marine air masses (originating in the Austral Ocean and the deep ASL) compared to Mount Johns. The Mount Johns site is located inland in WA and thus was not influenced the same way by marine air masses. According to Thomas et al. (2013), the Ferrigno region has suffered isotopic warming since 1957, as observed in the δD record. This warming, along with the strengthening of the meridional wind flow from north to south, caused the advection of more humidity and heat to the drilling site (THOMAS et al., 2013).

Consequently, the Ferrigno region displayed a higher increase in temperatures during the study period (Figure 7c) because of the strengthening of cyclogenesis and deepening of the ASL in the Austral Ocean and a shift in the meridional wind anomaly from north to south (onshore). The Mount Johns drilling site did not show the same trend, being more influenced by cold, continental air masses coming from the Antarctic ice sheet. This conclusion is in agreement with Steig et al. (2009), who found a strong warming in the Antarctic Peninsula and WA since 1957 and a slight cooling in East Antarctica for the same period.

Generally, there was a positive anomaly in the MSLP in the Amundsen/Bellingshausen Seas during El Niño events and a negative anomaly during La Niña (TURNER, 2004). Furthermore, the teleconnection between the tropical Pacific and WA coastal region was weak during the summer and strengthened in winter, influencing the depth of the ASL (TURNER et al., 2013; CLEM et al., 2017). Thereby, a decrease in atmospheric flux from the Austral Ocean to the interior of the WA during the winter season, caused by the propagation of the ENSO signal (El Niño), could also have contributed to the reduction in Na^+ concentrations in the last decades at the Mount Johns drilling site (Figure 11).

Therefore, the WA coastal region was influenced more by relatively warm air masses, mainly since the 1960s. As a result, the ice mass balance was altered, becoming more negative (WA losing ice), caused by an increase in ice flow from the continent to the sea, thus contributing to an increase in the global mean sea level. As a result, the WAIS is potentially unstable and becomes thinner in the Amundsen Sea region (BROMWICH et al., 2013; MAYEWSKI et al., 2017).

Figure 11 – Correlation between ERA-Interim (ECMWF) sea ice concentration in the Austral Ocean and sodium (Na^+) from the Mount Johns ice core (green triangle) for 1979–2008 at a 0.95 significance level.

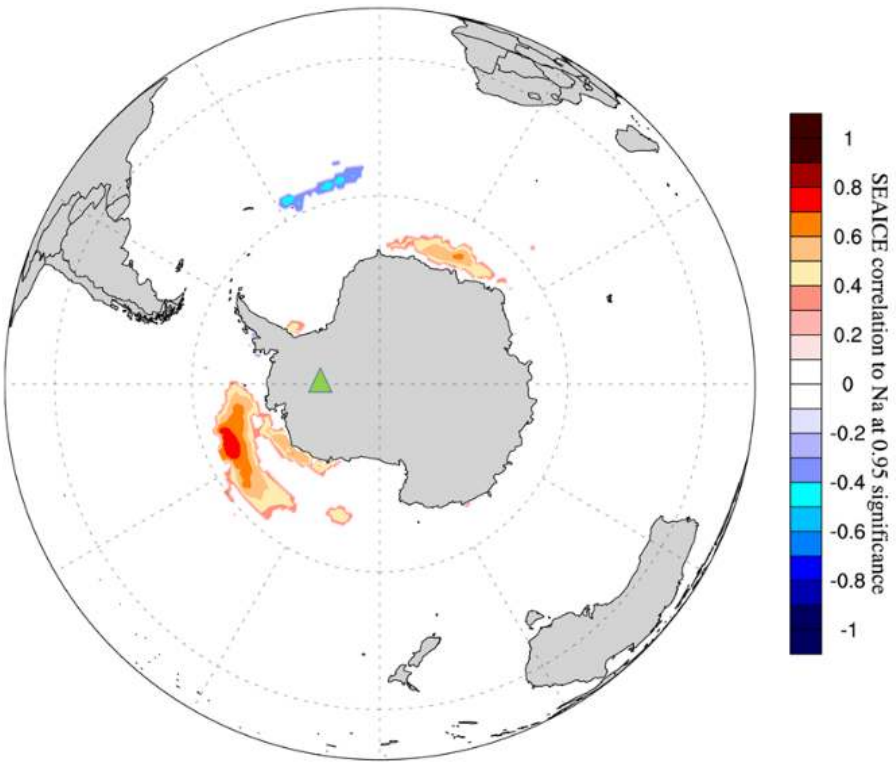

Source: CCI-U.MAINE / ECMWF / CPC-UFRGS.

CONCLUSIONS

This work shows the climate evolution of the South Pacific Ocean from 1900 to 2010 and its influence on the West Antarctica climate, using ERA-20C climatic reanalysis (ECMWF) and data from two ice cores (Mount Johns and Ferrigno).

The results show an increase in the sea surface temperature of the Pacific Ocean of + 0.007 °C yr^{-1} in the equatorial Pacific and + 0.008 °C yr^{-1} in the South Pacific intermediate latitudes. These changes have been associated with a positive trend in Southern Annular Mode since around the 1960s, along with the increase in sea surface temperature; a change in the mean sea level pressure anomaly signal also occurred in the South Pacific Ocean in the same period. This resulted in an increase in atmospheric pressure at intermediate latitudes and a reduction around Antarctica and the Austral Ocean, which strengthened the Amundsen Sea Low.

This change in atmospheric pressure signal and deepening of the Amundsen Sea Low altered the meridional wind anomaly at 850 hPa between the intermediate and high latitudes of the South Pacific Ocean in the 1960s. From that time onward, a higher north-south flow (onshore) predominated from the southeast South Pacific Ocean toward the West Antarctic (Figure 12).

Figure 12 – Differences in the annual sea surface temperature (SST, in °C) between (a) 1900–1920 and (b) 2001–2010, the blue star indicates the site with the highest increase in SST in the SPO (40° S, 150° W); differences in the mean sea level pressure (MSLP, in hPa) anomaly between (c) 1900–1920 and (d) 2001–2010, Amundsen Sea Low (ASL); differences in the annual meridional wind (v) anomaly between (e) 1900–1920 and (f) 2001–2010.

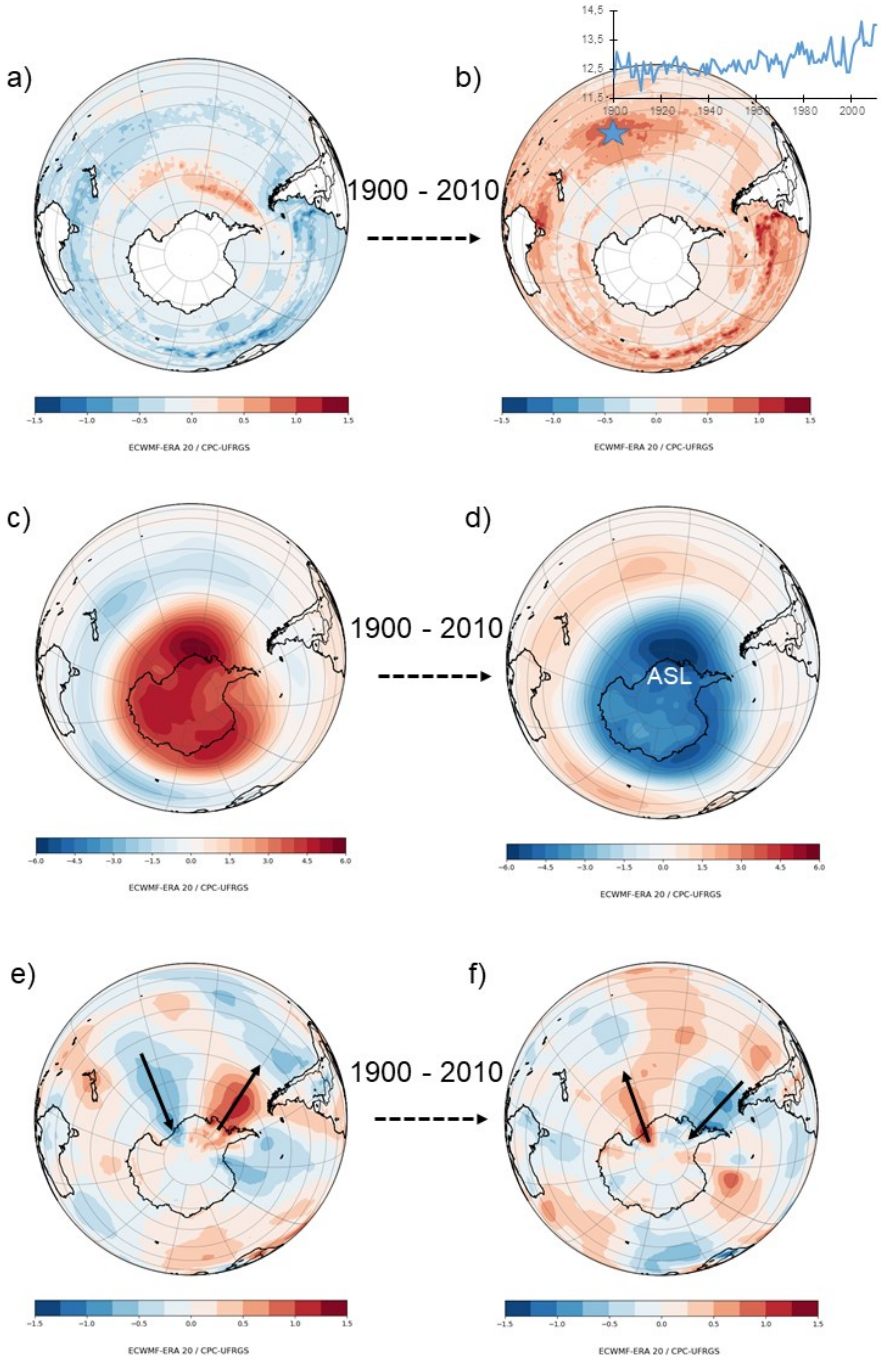

Source: ECMWF / CPC-UFRGS.

This atmospheric condition caused an increase in the flow of warm and humid air from the southeast South Pacific Ocean to the west of the West Antarctic, reducing the sea ice extent in the Amundsen/Bellingshausen Seas and increasing the atmospheric temperature

(mainly in the coastal West Antarctic, where the Ferrigno site is located). The Mount Johns site had a minor increasing trend due to its location (further inland than Ferrigno), where cold air masses from the interior of Antarctica have a stronger influence than do coastal air masses.

ACKNOWLEDGEMENTS

J. M. Dalla Rosa thanks CAPES for his PhD grant. This article is a contribution from INCT da Criosfera) to the Brazilian Antarctic Program – PROANTAR (CNPq project 465680/2014-3, MCTI/CNPq/CAPES/FAPS Nº 16/2014 - PROGRAMA INCT).

REFERENCES

ABRAM, N. J.; MULVANEY, R.; VIMEUX, F.; PHIPPS, S. J.; TURNER, J.; ENGLAND, M. H. Evolution of the Southern Annular Mode during the past millennium. **Nature Climate Change**, vol. 4, no. 7, p. 564–569, 2014. https://doi.org/10.1038/nclimate2235.

BERRISFORD, P.; DEE, D.; POLI, P.; BRUGGE, R.; FIELDING, K.; FUENTES, M.; KALLBERG, P.; KOBAYASHI, S.; UPPALA, S.; SIMMONS, A. ERA Interim Descripition. **ERA report series**, 2011. Available at: http://www.ecmwf.int/publications/.

BROMWICH, D. H.; NICOLAS, J. P.; MONAGHAN, A. J.; LAZZARA, M. A.; KELLER, L. M.; WEIDNER, G. A.; WILSON, A. B. Central West Antarctica among the most rapidly warming regions on Earth. **Nature Geoscience**, vol. 6, no. 2, p. 139–145, 2013. DOI 10.1038/ngeo1671.

BROOK, E. J.; BUIZERT, C. Antarctic and global climate history viewed from ice cores. **Nature**, vol. 558, no. 7709, p. 200–208, 2018. DOI 10.1038/s41586-018-0172-5. Available at: http://dx.doi.org/10.1038/s41586-018-0172-5.

CHENG, L.; TRENBERTH, K. E.; FASULLO, J. T.; MAYER, M.; BALMASEDA, M.; ZHU, J. Evolution of ocean heat content related to ENSO. **Journal of Climate**, vol. 32, no. 12, p. 3529–3556, 2019. https://doi.org/10.1175/JCLI-D-18-0607.1.

CLEM, K. R.; RENWICK, J. A.; MCGREGOR, J. Large-scale forcing of the Amundsen Sea low and its influence on sea ice and west antarctic temperature. **Journal of Climate**, vol. 30, no. 20, p. 8405–8424, 2017. https://doi.org/10.1175/JCLI-D-16-0891.1.

DANSGAARD, W. Stable isotopes in precipitation. **Tellus**, vol. 16, no. 4, p. 436–468, 1964. https://doi.org/10.3402/tellusa.v16i4.8993.

DING, Q.; STEIG, E. J.; BATTISTI, D. S.; KÜTTEL, M. Winter warming in West Antarctica caused by central tropical Pacific warming. **Nature Geoscience**, vol. 4, no. 6, p. 398–403, 2011. DOI 10.1038/ngeo1129.

HOLLAND, D. M.; NICHOLLS, K. W.; BASINSKI, A. The Southern Ocean and its interaction with

the Antarctic Ice Sheet. **Science**, vol. 367, no. 6484, p. 1326–1330, 2020. https://doi.org/10.1126/science.aaz5491.

HOSKING, J. S.; ORR, A.; MARSHALL, G. J.; TURNER, J.; PHILLIPS, T. The influence of the amundsen-bellingshausen seas low on the climate of West Antarctica and its representation in coupled climate model simulations. **Journal of Climate**, vol. 26, no. 17, p. 6633–6648, 2013. https://doi.org/10.1175/JCLI-D-12-00813.1.

HU, Y.; HUANG, H.; ZHOU, C. Widening and weakening of the Hadley circulation under global warming. **Science Bulletin**, vol. 63, no. 10, p. 640–644, 30 May 2018. https://doi.org/10.1016/j.scib.2018.04.020.

HUDSON, R. D. Measurements of the movement of the jet streams at mid-latitudes, in the Northern and Southern Hemispheres, 1979 to 2010. **Atmospheric Chemistry and Physics**, vol. 12, no. 16, p. 7797–7808, 2012. https://doi.org/10.5194/acp-12-7797-2012.

INOUE, M.; CURRAN, M. A. J.; MOY, A. D.; VAN OMMEN, T. D.; FRASER, A. D.; PHILLIPS, H. E.; GOODWIN, I. D. A glaciochemical study of the 120 m ice core from Mill Island, East Antarctica. **Climate of the Past**, vol. 13, no. 5, p. 437–453, 2017. https://doi.org/10.5194/cp-13-437-2017.

JONES, J. M.; FOGT, R. L.; WIDMANN, M.; MARSHALL, G. J.; JONES, P. D.; VISBECK, M. Historical SAM variability. Part I: Century-length seasonal reconstructions. **Journal of Climate**, vol. 22, no. 20, p. 5319–5345, 2009. https://doi.org/10.1175/2009JCLI2785.1.

LEGRAND, M.; MAYEWSKI, P. Glaciochemistry of polar ice cores: A review. **Reviews of Geophysics**, vol. 35, no. 3, p. 219–243, 1997. https://doi.org/10.1029/96RG03527.

LIU, Z.; ALEXANDER, M. Atmospheric bridge, oceanic tunnel, and global climatic teleconnections. **Reviews of Geophysics**, vol. 45, no. 2, p. 1–34, 2007. https://doi.org/10.1029/2005RG000172.

MARSHALL, G. J. Trends in the Southern Annular Mode from observations and reanalyses. **Journal of Climate**, vol. 16, no. 24, p. 4134–4143, 2003. https://doi.org/10.1175/1520-0442(2003)016<4134:TITSAM>2.0.CO;2.

MARSHALL, G. J.; ORR, A.; VAN LIPZIG, N. P.M.; KING, J. C. The impact of a changing Southern Hemisphere Annular Mode on Antarctic Peninsula summer temperatures. **Journal of Climate**, vol. 19, no. 20, p. 5388–5404, 2006. https://doi.org/10.1175/JCLI3844.1.

MAYEWSKI, P. A.; CARLETON, A. M.; BIRKEL, S. D.; DIXON, D.; KURBATOV, A. V.; KOROTKIKH, E.; MCCONNELL, J.; CURRAN, M.; COLE-DAI, J.; JIANG, S.; PLUMMER, C.; VANCE, T.; MAASCH, K. A.; SNEED, S. B.; HANDLEY, M. Ice core and climate reanalysis analogs to predict Antarctic and Southern Hemisphere climate changes. **Quaternary Science Reviews**, vol. 155, p. 50–66, 2017. DOI 10.1016/j.quascirev.2016.11.017.

MAYEWSKI, P. A.; MAASCH, K. A.; DIXON, D.; SNEED, S. B.; OGLESBY, R.; KOROTKIKH, E.; POTOCKI, M.; GRIGHOLM, B.; KREUTZ, K.; KURBATOV, A. V.; SPAULDING, N.; STAGER, J. C.; TAYLOR, K. C.; STEIG, E. J.; WHITE, J.; BERTLER, N. A. N.; GOODWIN, I.; SIMÕES, J. C.; JAÑA, R.; … FASTOOK, J. West Antarctica's sensitivity to natural and human-forced climate change over the Holocene. **Journal of Quaternary Science**, vol. 28, no. 1, p. 40–48, 2013. https://doi.org/10.1002/jqs.2593.

NICOLAS, J. P.; BROMWICH, D. H. Climate of West Antarctica and influence of marine air intrusions. **Journal of Climate**, vol. 24, no. 1, p. 49–67, 2011. https://doi.org/10.1175/2010JCLI3522.1.

PETIT, J. R.; JOUZEL, J.; RAYNAUD, D.; BARKOV, N. I.; BARNOLA, J. M.; BASILE, I.; BENDER, M.; CHAPPELLAZ, J.; DAVIS, M.; DELAYGUE, G.; DELMOTTE, M.; KOTIYAKOV, V. M.; LEGRAND, M.; LIPENKOV, V. Y.; LORIUS, C.; PÉPIN, L.; RITZ, C.; SALTZMAN, E.; STIEVENARD, M. Climate and atmospheric history of the past 420,000 years from the Vostok ice core, Antarctica. **Nature**, vol. 399, no. 6735, p. 429–436, 1999. https://doi.org/10.1038/20859.

POLI, P.; HERSBACH, H.; DEE, D. P.; BERRISFORD, P.; SIMMONS, A. J.; VITART, F.; LALOYAUX, P.; TAN, D. G.H.; PEUBEY, C.; THÉPAUT, J. N.; TRÉMOLET, Y.; HÓLM, E. V.; BONAVITA, M.; ISAKSEN, L.; FISHER, M. ERA-20C: An atmospheric reanalysis of the twentieth century. **Journal of Climate**, vol. 29, no. 11, p. 4083–4097, 2016. https://doi.org/10.1175/JCLI-D-15-0556.1.

POLI, P.; HERSBACH, H.; TAN, D.; DEE, D.; THÉPAUT, J. N.; SIMMONS, A.; PEUBEY, C.; LALOYAUX, P.; KOMORI, T.; BERRISFORD, P.; DRAGANI, R.; TRÉMOLET, Y.; HŐLM, E.; BONAVITA, M.; ISAKSEN, L.; FISHER, M. ERA report series: The data assimilation system and initial performance evaluation of the ECMWF pilot reanalysis of the 20th-century assimilating surface observations only (ERA-20C). , p. 1–62, 2015.

RAPHAEL, M. N.; MARSHALL, G. J.; TURNER, J.; FOGT, R. L.; SCHNEIDER, D.; DIXON, D. A.; HOSKING, J. S.; JONES, J. M.; HOBBS, W. R. The Amundsen sea low: Variability, change, and impact on Antarctic climate. **Bulletin of the American Meteorological Society**, vol. 97, no. 1, p. 111–121, 2016. https://doi.org/10.1175/BAMS-D-14-00018.1.

SCHWANCK, F.; SIMÕES, J. C.; HANDLEY, M.; MAYEWSKI, P. A.; AUGER, J. D.; BERNARDO, R. T.; AQUINO, F. E. A 125-year record of climate and chemistry variability at the Pine Island Glacier ice divide, Antarctica. **Cryosphere**, vol. 11, no. 4, p. 1537–1552, 2017. https://doi.org/10.5194/tc-11-1537-2017.

SIMÕES, J. C. Glossário da língua portuguesa da neve, do gelo e termos correlatos. **Pesquisa Antártica Brasileira**, vol. 4, p. 119–154, 2004. Available at: http://ftp2.cnpq.br/pub/doc/proantar/pab-12.pdf.

STEIG, E. J.; DING, Q.; WHITE, J. W.C.; KÜTTEL, M.; RUPPER, S. B.; NEUMANN, T. A.; NEFF, P. D.; GALLANT, A. J.E.; MAYEWSKI, P. A.; TAYLOR, K. C.; HOFFMANN, G.; DIXON, D. A.; SCHOENEMANN, S. W.; MARKLE, B. R.; FUDGE, T. J.; SCHNEIDER, D. P.; SCHAUER, A. J.; TEEL, R. P.; VAUGHN, B. H.; … KOROTKIKH, E. Recent climate and ice-sheet changes in West Antarctica compared with the past 2,000 years. **Nature Geoscience**, vol. 6, no. 5, p. 372–375, 2013. DOI 10.1038/ngeo1778.

STEIG, E. J.; SCHNEIDER, D. P.; RUTHERFORD, S. D.; MANN, M. E.; COMISO, J. C.; SHINDELL, D. T. Warming of the Antarctic ice-sheet surface since the 1957 International Geophysical Year. **Nature**, vol. 457, no. 7228, p. 459–462, 2009. DOI 10.1038/nature07669.

THOEN, I. U.; SIMÕES, J. C.; LINDAU, F. G. L.; SNEED, S. B. Ionic content in an ice core from the West Antarctic Ice Sheet: 1882–2008 A.D. **Brazilian Journal of Geology**, vol. 48, no. 4, p. 853–865, 2018. https://doi.org/10.1590/2317-4889201820180037.

THOMAS, E. R.; HOSKING, J. S.; TUCKWELL, R. R.; WARREN, R. A.; LUDLOW, E. C. Twentieth century increase in snowfall in coastal West Antarctica. **Geophysical Research Letters**, vol. 42, no. 21, p. 9387–9393, 2015. https://doi.org/10.1002/2015GL065750.

THOMAS, E. R.; BRACEGIRDLE, T. J.; TURNER, J.; WOLFF, E. W. A 308 year record of climate variability in West Antarctica. **Geophysical Research Letters**, vol. 40, no. 20, p. 5492–5496, 2013. https://doi.org/10.1002/2013GL057782.

THOMPSON, D. W. J.; SOLOMON, S. Interpretation of recent Southern Hemisphere climate change. **Science**, vol. 296, no. 5569, p. 895–899, 2002. https://doi.org/10.1126/science.1069270.

THOMPSON, D. W. J.; SOLOMON, S.; KUSHNER, P. J.; ENGLAND, M. H.; GRISE, K. M.; KAROLY, D. J. Signatures of the Antarctic ozone hole in Southern Hemisphere surface climate change. **Nature Geoscience**, vol. 4, no. 11, p. 741–749, 2011. DOI 10.1038/ngeo1296.

TRENBERTH, K. E. Changes in precipitation with climate change. **Climate Research**, vol. 47, no. 1–2, p. 123–138, 2011. https://doi.org/10.3354/cr00953.

TURNER, J. The El Niño-Southern Oscillation and Antarctica. **International Journal of Climatology**, vol. 24, no. 1, p. 1–31, 2004. https://doi.org/10.1002/joc.965.

TURNER, J.; COMISO, J. C.; MARSHALL, G. J.; LACHLAN-COPE, T. A.; BRACEGIRDLE, T.; MAKSYM, T.; MEREDITH, M. P.; WANG, Z.; ORR, A. Non-annular atmospheric circulation change induced by stratospheric ozone depletion and its role in the recent increase of Antarctic sea ice extent. **Geophysical Research Letters**, vol. 36, no. 8, p. 1–5, 2009. https://doi.org/10.1029/2009GL037524.

TURNER, J.; PHILLIPS, T.; HOSKING, J. S.; MARSHALL, G. J.; ORR, A. The amundsen sea low. **International Journal of Climatology**, vol. 33, no. 7, p. 1818–1829, 2013. https://doi.org/10.1002/joc.3558.

WOLFF, E. W. Chemical signals of past climate and environment from polar ice cores and firn air. **Chemical Society Reviews**, vol. 41, no. 19, p. 6247–6258, 2012. https://doi.org/10.1039/c2cs35227c.

WOLFF, E. W.; RANKIN, A. M.; RÖTHLISBERGER, R. An ice core indicator of Antarctic sea ice production? **Geophysical Research Letters**, vol. 30, no. 22, p. 2–5, 2003. https://doi.org/10.1029/2003GL018454.

YUAN, X.; KAPLAN, M. R.; CANE, M. A. The interconnected global climate system-a review of tropical-polar teleconnections. **Journal of Climate**, vol. 31, no. 15, p. 5765–5792, 2018. https://doi.org/10.1175/JCLI-D-16-0637.1.